

# INVESTIGATING THE AUTOROTATIONAL PERFORMANCE OF SCALED SAMARA ROTOR IN VERTICAL AND FORWARD FLIGHT

Mr Byungkwon Jung<sup>1</sup>, Dr Djamel Rezgui<sup>2</sup>

Department of Aerospace Engineering, University of Bristol, Queen's Building, University Walk, Bristol, BS8 1TR, UK

<sup>1</sup> PhD Student, [bj1798@my.bristol.ac.uk](mailto:bj1798@my.bristol.ac.uk)

<sup>2</sup> Lecturer in Aerospace Engineering, [djamel.rezgui@bristol.ac.uk](mailto:djamel.rezgui@bristol.ac.uk)

## ABSTRACT

Samara seeds are nature's most efficient fliers, they can create twice the lift compared to translating wings by the creation of the Leading edge vortex (LEV). Realising this, numerous Samara inspired UAVs are being created. However, a number of research questions still need to be answered to be able to harness the benefit of the LEV for UAV applications. In particular, if scaling up the natural Samara degrades its aerodynamics performance and how well the scaled Samara wings perform in autorotation in both the forward and vertical flight regimes. This paper explores the effects of scaling by a series of drop tests and wind tunnel tests. It was found that the vertical aerodynamic performance of the Samara wing starts degrading as its scale reaches a ratio of 8:1 size to the natural Samara seed. In terms of forward flight, the natural Samara found it hard to cope with any slight deviations from vertical descent whereas the artificial scaled Samara were able to autorotate up to 80 degrees shaft angle relative to the wind direction. The effect of scaling in forward flight was also explored; a 1:1 to 4:1 scaling boosted the thrust by around seven folds whereas a 4:1 to 8:1 scaling increased the thrust by four times.

Key words: Samara seed, maple seed, leading edge vortex (LEV), small rotor, autorotation.

## 1 INTRODUCTION



Figure 1: Example of past developed UAVs. Left: Lockheed Martin SAMARAI [1]. Right: University of Maryland Monocopter [2]

Samara seeds are said to be nature's most efficient fliers. Using the phenomenon of autorotation, Samara seeds are capable of creating about twice the lift compared to

translating wings, whilst operating at angles of attack well above the conventional helicopter blades [3]. Realising such potential of Samara seeds, numerous Samara inspired UAVs have been introduced recently with its applications ranging from UAVs for surveillance, military (SAMARAI) [1] and even for exploring other planetary atmospheres [4]. See examples in Figure 1.

However, if these UAVs are to be designed successfully, it is necessary to look deeper into the unexplored characteristics of the natural Samara. For that reason, this study aims to answer two questions – “Does scaling up the natural Samara degrades its aerodynamic performance?” and “How does the scaled

autorotating Samara wing perform in the forward flight regime?"

For the Samara inspired UAVs, gaining and insight into the effects of scaling can be of great importance. As it can be used for the design of samara inspired rotors capable of producing the required lift at the desired descent speeds and for the given payload.

### 1.1 Background

A Samara is a type of dry fruit where the seed is enveloped by a papery tissue that helps the seed to drift away from a tree [5]. (Figure 2) Typically in windy conditions, the Samara seed falls from the tree and they begin to autorotate. This autorotation generates lift that prolongs the descent of the seed. By further relying upon wind and up-gust, the seed is widely dispersed; travelling distance ranging from several metres to kilometres from the parent tree [5, 6].



Figure 2 Photographs of maple seeds [17]

Various trees produce such winged seed; from elm, ash, maple and sycamore [6]. Hence, sometimes Samara seeds are referred to as maple seeds or sycamore seeds. In nature, numerous varieties of Samaras seeds exist. One familiar type is the doubled wing Samara found on maple trees. Ash tree, on the other hand, has a single elongated wing and Triplaris tree disperses its seeds by means of a three-winged "flying" fruit [6, 7].

Each Samara seed also has its own specific mass, size, roughness and shape; thus giving a unique aerodynamic performance. But, widely speaking, most Samara seeds are a few centimetres in span, record terminal velocities of under 1m/s and have flight Reynolds numbers of

around 1000 [8]. Most seeds have the heavy nut, i.e. the centre of mass, positioned at the base and this gives the screw-like rotation. Despite of the small wing area, by this rotation, the Samara seed is renowned for creating extraordinarily high lift and this feat have caught the attention of many researchers.

### 1.2 Leading Edge Vortex

The extra lift of the Samara wing comes from the mechanism known as the leading edge vortex (LEV). The leading edge vortex is essentially a tornado-like vortex that sits on top of the leading edge. This vortex generates an enhanced circulation and consequently creates a region of low pressure above the wing. This low pressure in-turn results in the 'extra lift'. By generating this LEV, autorotating Samara seeds are capable of creating about twice the lift and also drag compared to translating wings [3].

Lentink tried to visually check the existence of the LEV of Samara seeds. By building a dynamically scaled seed model made of transparent acrylic and testing it in a tank of mineral oil, Lentink successfully constructed a 3D velocity field around various model seeds when autorotating. By this, He discovered that prominent LEV was formed near the base for all model seeds (25% Span). And towards the tip, the LEV merged with the tip vortex (75% Span) to shed as wake [6].

Using a vertical wind tunnel and by filming freely flying 34 Samara seeds, Lentink found out that autorotating natural seeds also generate a prominent stable LEV near their base. More importantly, he found out that the structure of the LEV depended on the Reynolds number ( $Re$ ), the Samara shape and especially, on the Samara seed's angle of attack. Furthermore, the natural seeds flew at wing tip angles varying from  $12^\circ$  to  $32^\circ$ . The hornbeam seeds with high tip angle produced a more separated LEV in comparison to maple seeds with low tip angle which produced a compact, stable LEV [6].

Lentink also computed the lift coefficient distribution along the maple and hornbeam seed's span by integrating the vortices. The sectional lift coefficient reaches very high values

from 2 for horn beam seed to 5 for maple seeds. This is predominantly due to the angles of attack: at the root the angle of attack can reach 90 degrees, whereas at the tip, it is reduced to 30 degrees [6]. It is worth noting that the angle of attack is well beyond the stall point for conventional aircraft wings and helicopter blades, but the LEV is still attached [6].

The LEV is also found in many of the nature's fliers like hawk moth, butterflies and fruit flies [3, 9]. The LEV structure and lift coefficient distribution found in the maple seed by Lentink was similar to the results found in fruit flies [10, 11]. In addition, for insect wings operating at Reynolds number of the same order of 100 to 1000, the attachment of LEV depended on the strong spanwise flow on the top of the wing. The spanwise flow is said to stretch the LEV so that it does not break up but tightens [10].

This statement that strong spanwise flow stabilises the LEV is supported by a study by Salcedo who conducted a stereoscopic particle image velocimetry (DPIV) of a descending mahogany seed in a vertical wind tunnel [12]. He found that the presence of strong spanwise flow produced by centrifugal forces helps the LEV to stretch, thus increasing its intensity and promoting it to attach to the aerofoil. This strong spanwise flow is said to produce a steep increase in pressure differential and thus create the extra lift of the LEV.

Lentink and Dickinson, in particular, investigated the LEV of revolving fruit-fly wing by performing flow measurements and visualisations in water tank by employing air bubbles. They found out that LEV is stabilized by the 'quasi-steady' centripetal and Coriolis accelerations that is present at low Rossby number ( $Ro$ )<sup>1</sup>. It is favourable to have low wing aspect ratio and high rate of rotation. The Reynolds number ( $Re$ ) in comparison only seemed to affect the structure of the LEV [3].

For example, a wing operating at high  $Re$  resulted in the vortex to burst but the LEV was still stable and no reduction in lift was apparent.

---

<sup>1</sup> Rossby Number is the ratio of radius of blade gyration to blade chord.

However, if the Rossby number rose above the critical number of three, the rotating fly wing's LEV started to separate and grew unstable. Hence, a rise in Rossby number reduces the lift and drag coefficients. In fact, they calculated that the Rossby number for over 300 single wings from insect, birds, bats, seeds and fins of fish. The Rossby number, not surprisingly, all seemed to be close to three [3].

Furthermore, Lentink and Dickinson highlighted the importance of spanwise flow. They support the hypothesis that spanwise flow balances the formation of vorticity at the leading edge and drains it into the tip vortex. Low Rossby number helps the spanwise flow as Rossby number is also a measure of inertial to Coriolis forces [3].

In 2015, Limacher suggested that the tip speed ratio is critical for LEV stabilisation [13]. By abstracting the natural Samara flight with a rotating plate in free stream, and by using Particle image velocimetry for visualisation, Limacher showed that tip speed ratio causes a transition of the mean wake topology from bluff body to stable leading edge vortex. This is because, the increased tip speed ratio, creates a spanwise flow that stretches the vortex and creates a compact leading edge vortex. However, the exact boundary of the topological transition was not known [13].

Although the tip speed ratio is responsible for the LEV, they found that the tip speed ratio has negligible effect on the leading edge circulation at the same spanwise position, local effective angle of attack and local effective velocity.

So it seems that tip speed ratio, low Rossby number is important so that spanwise flow is possible and LEV remains stable and compact. However, the question of how big can we make the Samara inspired blade remains unanswered.

Rather than looking into the physics of the Samara seed, i.e. the LEV, Azuma and Yasuda [14] tried to understand the aerodynamics of the Samara seed through creating and testing various wing models. They in particular, looked

into the visible characteristics of the seed like the rate of descent ( $V$ ), the rotational speed ( $\Omega$ ), the coning angle ( $\beta$ ) and the feathering angle ( $\theta$ ) of the seed and from this they found out that all of these parameters were unsurprisingly coupled [15].

By using a vertical wind tunnel, Yasuda et al found the wind speed to make the spinning seed to float in the test section; this gave the vertical rate of descent speed and the other parameters were measured using a stroboscope and a camera. From this it was observed that natural Samara had a low rate of descent ( $\approx 1\text{m/s}$ ) and this is driven by the high rotational speed (1000rev/min) and low coning angle ( $\approx 10^\circ$ ) [14].

Also, by creating Samara models, Yasuda confirmed that the centre of mass position was critical in ensuring autorotation. It had to be near the root of the seed. Yasuda also found out properties of the natural seed that promotes low descent rate, high rotational speed and low coning angle [15].

Firstly, thick leading edge and roughness, seen in real seed, was critical. The ribbed surface structure of the natural Samara not only improved the aerodynamics but kept the centre of gravity forwards, to give more stability. Removing these surface irregularities gave a 15 percent reduction in the spin rate. As for the leading edge, a single thin circular glass fibre attached to the leading edge of the balsa wing gave a 30 percent reduction in the rate of descent. Secondly, the wing required a negative camber (i.e. bent convex upwards) as this helped the aerofoil to be stable for changes in the angle of attack [15].

Yasuda and Azuma on the other hand, concluded that the negative camber near to the root, the pattern (surface roughness) of the fibrous wing, and the leading edge extra thickness close to the root lead to the enhanced aerodynamic characteristics observed in samara seeds, suggesting that they may play a key role in the stability of LEVs [15].

Following up from the above studies, the main goal of current study is to investigate the effect

of scaling up the Samara seed on its autorotational performance, in both vertical and forward flight regimes. The study hopes to add further understanding to stability of the LEV.

## 2 Methodology

This section summarises the methodology used in this study. First, artificial Samara wings had to be built and their performance had to be assessed. Five Samara wings were made for each scale of 1:1, 4:1 and 8:1. Care and attention were given in building every new Samara wing, to optimise the wings to the best standard by using information from Azuma and Yasuda [14] and by means of trial and error. Out of each five samples, the best Samara wing was selected and its vertical performance was measured by conducting a series of drop tests. The drop tests used a high speed camera to capture the vertical descent of the Samara wing. The tests were only carried out in the vertical sense, as this was the simplest and the most effective way of measuring the autorotational performance.

A numerical analysis of the scaled Samara wing in vertical descent was also conducted. It combined the momentum and blade element theory, to predict the performance of the scaled Samara wing, if the LEV was still stable and attached. Performance parameters like the rate of descent for given disc loading were compared for both the drop test and numerical analysis. This was used to indicate the possibility of the LEV presence.

Wind tunnel tests were carried out to extend the analysis in the vertical decent condition and determine the forward flight performance of scaled Samaras. However, instead of using a single wing Samara, two wings were connected together to construct a rotor. This setup was chosen as it was difficult for single winged rotors to enter into autorotation with an edgewise wind component, i.e. forward flight condition. In the wind tunnel tests, the thrust of the rotor was measured for varying flow speeds and rotor shaft tilt angles. The obtained results were also used in the validation of the numerical performance code.

The methodology of the current study was therefore divided into four parts:

- ①. Construction of scaled Samara wings.
- ②. Vertical drop tests of scaled Samara wings.
- ③. Wind tunnel test of scaled Samara rotors.
- ④. Numerical Analysis of scaled Samara wings or rotors.

## 2.1 Construction of scaled Samara wings

For the investigation, scaled Samara wings had to be built first. The shape and the dimension of the Samara wing was based on the Samara seed known as *Acer diabolicum* Blume. (Figure 3). This particular seed recorded the slowest descent rate along with the best lift distribution, making it as an ideal seed to base the artificial Samara wings on. As for the material, balsa wood was selected as it was the closest material to the Samara. So balsa wood Samara wings were built to a scale of 1:1, 4:1, and 8:1.

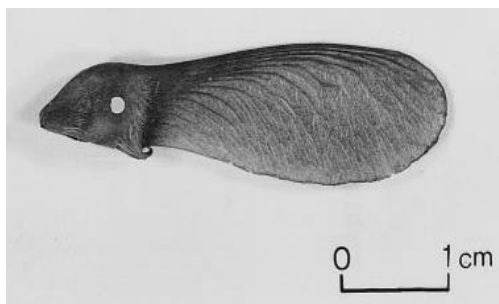


Figure 3. Photograph of the Blume Samara Seed [15]

When scaling and building the artificial Samara rotor, the following rules below were applied:

- **Span and chord:** “Main scaling parameter”. 4:1 means enlarging the span, chord, thickness of the seed by four times and 8:1 means eight times.
- **Leading edge thickness:** “Leading edge thickness to chord ratio ( $t/c$ ) must be around 4%” [16].

The seed’s leading edge thickness has a profound effect on the formation and the stability of the LEV. Lentink [16] created balsa Samara rotors and found that at a  $t/c$  ratio of 4%, the most stable and developed LEV was produced. As leading edge thickness thinned, the LEV became smaller and if the thickness became too

thick ( $>4\%$ ), an unstable LEV was created. To model this, thin circular wire was attached at the leading edge.

- **Thin skin:** “Sanding all the wing except the leading edge”

The natural Samara has very thin thickness except at the leading edge – The natural seed has a leading edge thickness of 0.42mm whereas at the trailing edge its thickness is 0.05mm. So, it was important to keep the artificial Samara as thin as possible except for the leading edge. Thus, it was sanded down.

- **Roughness:** “Adding secondary thin circular wires”

The natural seed has roughness inherently built in via vines (as in Figure 3). This roughness was found to aid the rate of rotation [15]. To gain a similar effect, two additional circular wires were placed on the artificial Samara wing. These wires differed in that they were half the thickness of the ones placed on the leading edge. The decision for two wires was based on trial and error from drop testing.

- **Negative camber:** “Force was applied to bend the flexible balsa Samara into negative camber”

- **CG position:** “Adding mass until the CG position is near the root”

Mass was added to the root to initially move the CG position near the root, then using repeated free falling test the mass was moved until optimum state of autorotation was achieved.

Figure 3 displays the parameters of the natural and single bladed Samara wings with the modifications made. Photographs of scaled Samara wings made are illustrated in Figure 4.

Dimensional differences between the natural and 1:1 scale model was due to modelling errors. The 1:1 model also has a much heavier mass – the natural Samara was too light to replicate and the balsa wood model required a greater mass to achieve autorotation. This was not a significant problem as disc loading was used instead of mass for comparing the natural and Samara models.

Table 1 Geometrical configurations of the natural Samara and scaled Samara wings

Parameters	Symbol	Unit	Blume (Theory) <sup>13</sup>	Natural (Test)	1:1	4:1	8:1
Rotor Radius	r	cm	3.62	4.5	3.9	15.3	30.0
Average chord length	c	cm	0.84	0.99	0.96	3.34	6.63
Radius of Gyration (~0.8r)	R	cm	2.90	3.6	3.12	$\frac{12.2}{4}$	24.0
Mass without blue-tack		grams	-	-	0.067	1.41	9.05
Mass with blue-tack	m	grams	0.058	0.130	0.260	4.71	21.08
Wing thickness (leading edge)		mm	-	-	0.1	0.8	1.6
Leading edge wire thickness		mm	-	-	0.315	0.5	1.2
Total leading edge thickness	t	mm	0.42	0.5	0.415	1.3	2.8
Thickness to chord ratio	t/c	%	5%	5%	4.3%	3.9%	4.2%

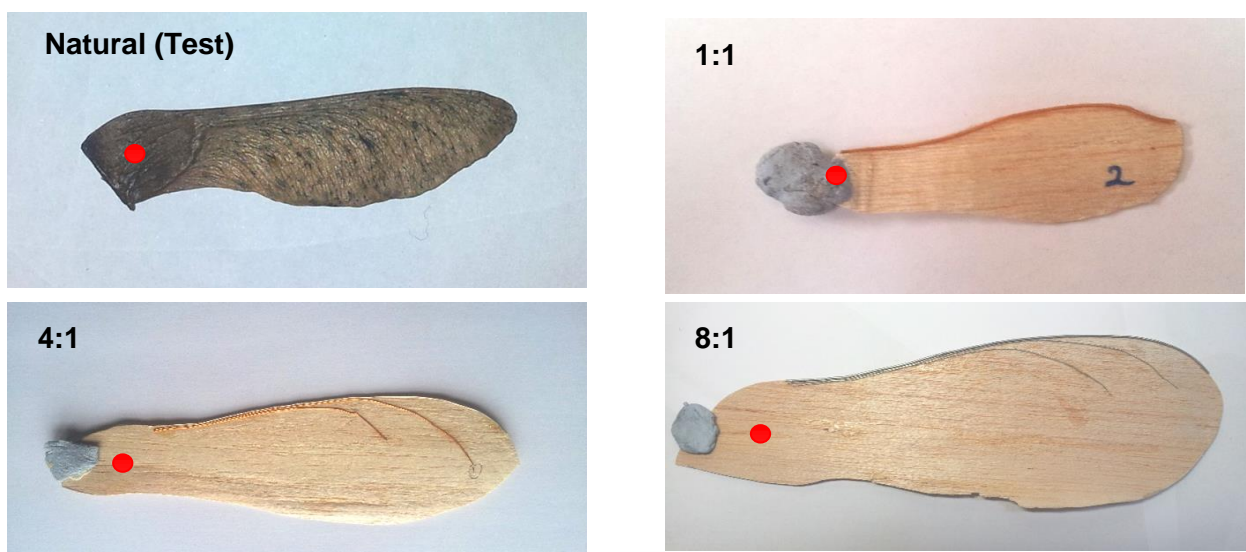


Figure 4 Photographs of the Samara wing models. The approximate centre of gravity positions are highlighted by a red circle. Blue-tack was used to allow shift changes in the centre of gravity

## 2.2 Vertical Drop test of Scaled Samara

With the Samara wings made the next step was to determine the characteristics or the vertical performance of the natural and artificial Samara wings. So, a drop test was conducted to measure the flight dynamics.

For the drop test, the Samara was dropped in still air with long axis facing vertically downwards from a height of 3 metres and a high speed camera near the bottom captured the descent, at a rate of 5000 frames per second. Sufficient height was chosen to ensure that the Samara reached the autorotational regime before falling into the field of view of the camera. The multiple images obtained were then used to resolve the coning angle ( $\beta$ ), the rate of fall ( $V$ ) and also rate of spin ( $n$ ) of the Samara wing. A background

with a vertical scale of 10cm step was also placed to allow for rate of descent to be measured.

## 2.3 Wind tunnel test of Scaled Samara

In order to conduct the wind tunnel test with the natural and artificial Samara wings, a suitable rig had to be built first. Figure 5 is the diagram of the rig used for the wind tunnel testing. The experimental rig measures the thrust induced by the rotor via the two load cells attached at the front and the rear. Below are some brief descriptions of parts of the rig:

- ①. Two thin film load cells, each with a capacity of 0.4N shares the thrust created by the rotor. The far end of the load cell (the end

with the rotor) deflects downwards as thrust is induced by the rotor and corresponding strain is converted into voltage.

- ②. A simple hinge allows the rig to rotate and thus the desired shaft angles from  $0^\circ$  to  $90^\circ$  can be achieved. A protractor was placed for accurate rig rotation.
- ③. A pin is soldered to the metal bar and a rotor head is placed through the pin to allow for rotation. The soldered joint was sanded

down to allow for a very smooth interface and to minimise the friction.

- ④. The artificial and natural Samaras inserted into the rotor head and are bolted firmly using screws. A hint of superglue was applied around the joint to restrict the Samara rotors from moving out of place.

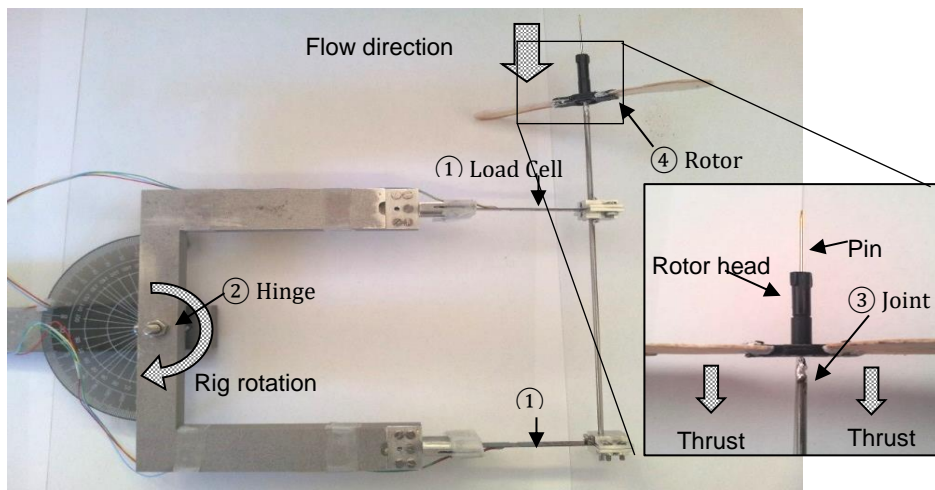


Figure 5. Photograph of the experimental rig with illustrations. The rotor is in  $0^\circ$  shaft angle, facing the flow. I.e. in vertical descent.

The strain gauge reading of the load cells had to be converted back to thrust. Before the wind tunnel experiment, a calibration graph of strain gauge reading vs. thrust graph was generated by placing weights and measuring the force.

The wind tunnel test was conducted in the return working section of the University of Bristol 7" by 5" low speed close loop wind tunnel. This tunnel was especially applicable to this particular experiment as Samara seeds operated at low speed and also any disturbances outside the wind tunnel was kept out. However, at low wind speeds (1 to 2m/s), the deviation in the wind speed was large (up to around 0.5m/s).

The rig was attached to a fixed stand inside the wind tunnel. Care was given to ensure that the rig was firmly fixed using a clamp as any unwanted vibratory movement will contribute to the load cell readings. The rig was set up horizontally so that the effects of gravity were minimal. A photograph of the set up can be seen in Figure 5.

Below is the brief description of how the experiment was carried out:

1. The rig was rotated to the desired angle and checks for any misalignment were made.
2. The rotor was inputted whilst making sure that the rig is secured
3. The strain gauge reader was then recalibrated
4. For each shaft angle from  $0^\circ$  to  $90^\circ$  (increments of  $10^\circ$ ), wind speed from 1m/s to 8m/s was tested with increments of 1m/s.
5. For each wind speed, three reading were taken for 1:1 scale rotor and the natural Samara. For the 4:1 and 8:1 scale Samara rotor, five reading were taken as the deviation in the reading was significant.
6. Once the rotor has reached 8m/s, the wind speed was slowly reduced by each step and the offset due to hysteresis was recorded
7. This was process was carried out for two bladed natural Samara, 1:1, 4:1 and 8:1 artificial Samara.

In terms of the test, one challenge was attaching the Samara wings to the rotor. The pitch and the twist of the Samara wing was inconsistent and this gave a different reading each test. To reduce the inconsistency, all Samara whether natural or artificial was bent to a similar pitch and twist as to the Natural Samara.

For 4:1 and 8:1 scale Samara rotors, the long span meant that the Samara wing began to flex. This gave large flapping and coning angles which was unreflective of Natural Samara. The 'Strain gauge readings' also deviated a lot for 4:1 and 8:1 scale rotors at high speeds. Sometimes up to around 0.3N which is about 30% of the total force measured. To account for such deviations more readings were taken for 4:1 and 8:1 scale models and the average was taken.

When the loads were high, friction between the rotor and the pin base, no longer was trivial. Oil was coated but this did not solve the problem.

#### 2.4 Numerical Analysis of scaled Samara

A simple numerical code that describes the autorotation performance of the Samara wing was written. The Matlab code incorporates the momentum theory and the blade element theory to give values for—the induced velocity ( $V_i$ ), rate of spin ( $\Omega$ ) and vertical descent ( $V_d$ ). As there were three unknowns, three equations were required:

1)  $\mathbf{T}_{B.E} - \mathbf{T}_m = \mathbf{0}$

Both blade element theory and momentum theory should give the same thrust.

2)  $\mathbf{Q}_{B.E} = \mathbf{0}$

Autorotation means the blade is spinning at constant rotational rate ( $\Omega$ ), with no input torque.

3)  $\mathbf{T}_{B.E} \sin(\theta) - \mathbf{W} = \mathbf{0}$

In autorotation and in vertical flight, the system is travelling at terminal velocity and has no acceleration giving vertical thrust must equal to weight.

The Matlab function `fsolve` was used to solve for the unknown values of  $V_i$ ,  $\Omega$  and  $V_d$ , for given set of parameters, for example, blade pitch, disc loading, etc. Simplifications have been made for both theories – the simple momentum theory assumes that the induced velocity is constant

over the blade span. 2D steady blade element theory was used with tip loss corrections. The blade aerofoil was represented by it characteristic lift and drag coefficients. Also, rather than having a constant mean chord, this code uses varying chord length across the span.

To make the code applicable to this investigation, the aerodynamic properties (lift curve slope, coefficient of drag) of the natural Samara must be defined. From literature, the lift coefficient of Samara seed can reach up to 5 at high angles of attack. However, this value was derived from the experimental LEV. Therefore, the LEV size and strength may vary considerably from time to time. To be more consistent, a lift coefficient curve proposed by Yasuda for the natural Blume Samara seed was used in this code [14]. This lift coefficient has a maximum lift coefficient at angle of attack of 20 degrees. (Figure 6)

To predict the lift curve slope and coefficient of drag, initial estimates for these values for the Blume Samara seed were obtained from Yasuda's report [14]. Then via an iterative process, these values were modified until the computed performances matched perfectly with the natural Samara's. ( $V=0.82\text{m/s}$ ,  $\Omega=977\text{ rev/min}$ ) This gave a value of lift curve slope of 3.90 and coefficient of drag of 0.115. In reality,  $C_d$  should change with angle of attack, but in this analysis, it was kept as constant for simplicity. With these aerodynamic properties defined, only the mass, chord distribution and wing radius had to be changed to get the natural Samara's performance at higher scales.

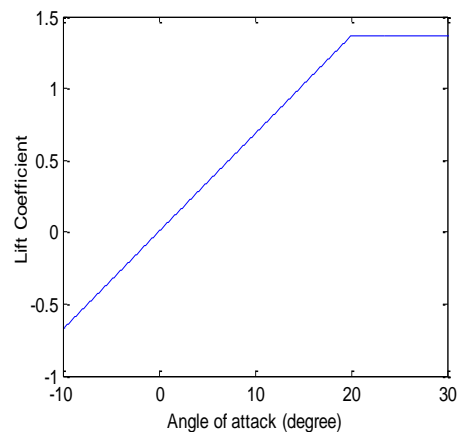


Figure 6 Lift coefficient curve to model the natural Samara



### 3 Results and Discussion

#### 3.1 Vertical Descent Results (Drop test)

Table 2 shows a higher descent rate for the model 1:1 Samara wing compared to the natural – the 1:1 model drops 45% faster than the natural, but this is most likely due to the heavier mass not poorer performance. To make a better comparison, disc loading versus the rate of descent graph was plotted (Figure 7). The red line is the minimum rate of descent in optimum state of operation and it's a guideline of the lowest descent rate possible. The blue line is the drop test result and the black line – the numerical. The numerical result will give a prediction of the performance of the autorotating Samara wing if the LEV still strong and attached. From Figure 7, the maple seeds and other natural Samara operate slightly above the optimum state of operation. The numerical result and the model results for 1:1 and 4:1 also run parallel to the red line. However, at the scale of 8:1, the modelled

wing no longer follows this line, but drifts away, suggesting that the wing no longer mimics the natural Samara. For 1:1 and 4:1 scale, the error in the descent rate between numerical and the model is very small at the same disk loading (6% and 8% respectively). But at the 8:1 scale, the error grows to 20%, and the result no longer matches. This suggest at 8:1 scale, effective LEV is no longer being produced. This sudden lost in LEV is surprising as the Rossby number (Radius of gyration/chord), for 8:1 scale, is lower than 3, implying the balsa wing should be able to produce stable LEV in theory. But, one reason for the lost in LEV may be due to the lack of rate of spin. At 8:1 scale, only 236 rev/min is achieved. This lack of spin may have limited the spanwise flow, making it harder for LEV to be sustained. In conclusion, it can be proposed that once the Samara wing radius reaches around 30cm (8:1), the LEV of the wing loses strength and higher rate of descent is experienced.

Parameters	Rate of descent (1 <sup>st</sup> seed)	Rate of descent (2 <sup>nd</sup> seed)	Disc loading	Rate of spin	Rossby number
Units	$V, \text{ms}^{-1}$	$V, \text{ms}^{-1}$	$\text{N/m}^2$	$\Omega, \text{rev/min}$	$\text{Ro}, R/c$
Blume Samara (Tuned)	0.82	-	0.22	977	2.15
Natural Samara (Test)	1.07	1.07	0.26	1000	2.15
Numerical Natural	1.03	-	0.26	980	2.15
Model 1:1	1.55	1.51	0.82	1460	2.03
Numerical 1:1	1.65	-	0.82	1736	2.03
Model 4:1	1.68	1.71	0.98	352	2.23
Numerical 4:1	1.81	-	0.98	505	2.23
Model 8:1	2.65	2.86	1.14	236	2.26
Numerical 8:1	2.09	-	1.14	275	2.26

Table 2 Results for experimental scaled Samara wing. The numerical code was tuned to the Blume Samara.

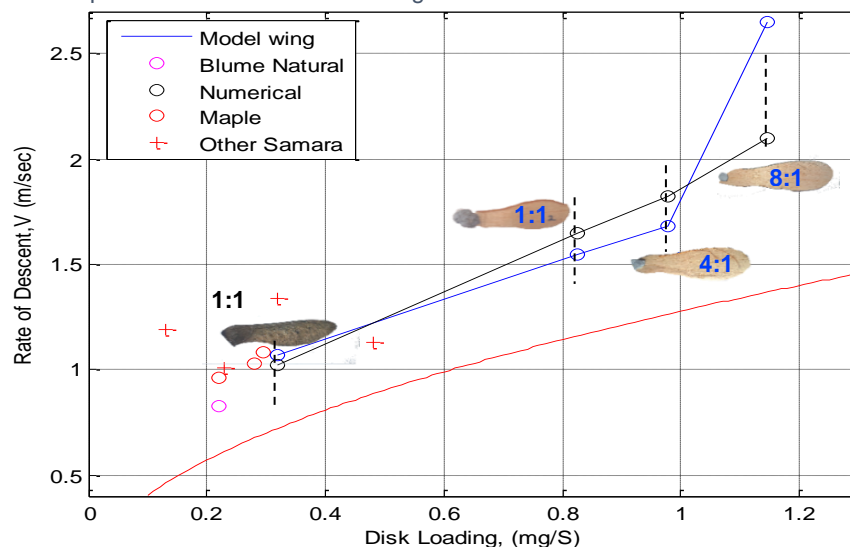


Figure 7. (Right) Rate of decent (m/s) versus Disk loading ( $\text{N/m}^2$ ) for natural, balsa wood scaled model wings and numerical solved scaled wings. The red line indicates the minimum rate at optimal state of autorotation.

However, there are always possibilities that other influences might have been responsible for this behaviour. One possibility is incorrect modelling. The balsa wing at 8:1 scale may not have been optimised to its full potential, leading to an offset in the result. One indication to that this may be true is the large coning angle. Normally, a coning angle of 10 to 20° is expected for maple seeds [8], but for 8:1 scale model wing, it was 27.5°. The feathering angle was also -7°, well above the average for Samara seeds of -1 to -3° [8]. This may imply that the balsa wing was not operating at its maximum potential. In fact, during testing, some concern was raised that the 8:1 scale Samara wing showed a boomerang-like motion rather than spinning on its axis. Other possibility is that the Samara wing might not have reached the auto-rotational regime fully when the results were taken - The wing being much bigger requires greater distance to reach auto-rotation. Therefore, some uncertainties still remain as to whether the LEV disappeared solely due to scaling.

### 3.2 Vertical Descent (Wind tunnel test)

Whilst conducting the Wind tunnel test, the vertical performance of the natural and artificial wings was obtained as it is when the shaft angle was set to 0°. By plotting thrust (N) versus the wind speed (m/s) trend at 0° shaft angle (refer to Figure 10-14), the thrust when the natural seed is in free fall autorotation can be calculated – this is when the wind speed is same as the vertical descent speed found in drop testing. With the thrust computed the disc loading can then be calculated. Table 3 contains all the results. The equivalent one bladed disc loading was obtained by halving the thrust of the two bladed rotor.

From Figure 9, an indicator of a stable LEV is when the results follow the red line known as the minimum rate of descent at optimal state of autorotation. Like previously mentioned, the drop test indicated by black line deviates from the red line at a scale of 8:1 suggesting the 8:1 scale Samara wing is not producing effective LEV. The same trend was observed for the wind tunnel test where clearly the purple and blue line seem to no longer run parallel to the red line at a scale of 8:1. Thus, even the wind tunnel test suggests that the 8:1 scale rotor is not producing effective LEV. Another feature is that the wind tunnel test shows a much greater disc loading than the drop test. This may be due to the fact that the two bladed Samara at the wind tunnel may have been operating at a different rate of rotation. If the plot is shifted to the left, we can get the same behaviour as the drop test.

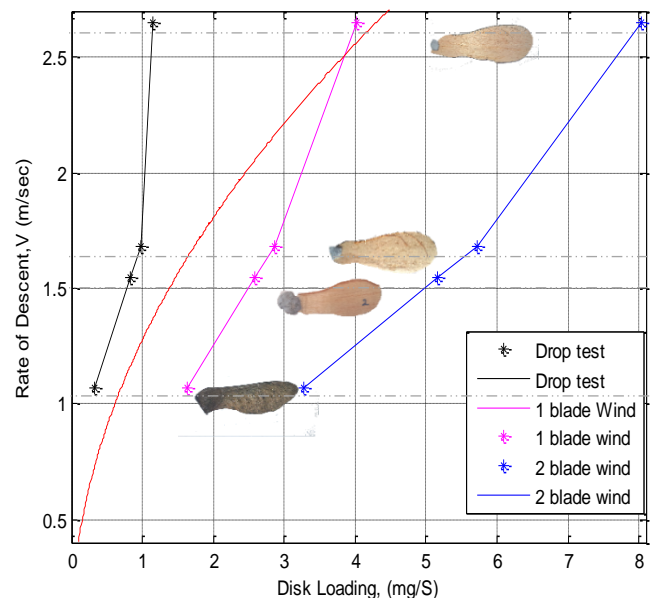


Figure 8 Graph showing rate of descent (m/s) vs. Disk loading (N/m<sup>2</sup>) for vertical descent of Samara wings in both the drop test and the wind tunnel test

Parameters	Rate of descent	Thrust for two bladed	S (Disk area)	Disc loading for two bladed	Disc loading for one bladed	Disc loading from drop test
Units	V, ms <sup>-1</sup>	N	m <sup>2</sup>	N/m <sup>2</sup>	N/m <sup>2</sup>	N/m <sup>2</sup>
Natural Samara (Test)	1.07	0.0134	0.0041	0.82	0.41	0.26
Model 1:1	1.55	0.0160	0.0031	5.162	2.581	0.82
Model 4:1	1.68	0.2664	0.0465	5.782	2.891	0.98
Model 8:1	2.65	1.456	0.1810	8.044	4.022	1.14

Table 3 Disc loading results from the wind tunnel test and from the drop test

### 3.3 Forward Flight Result

This section looks at the forward flight performance of two bladed scaled Samara rotors. For the graphs below model is the wind tunnel result and the numerical takes into account of the effects of the LEV. Hence, if the LEV is still effective, the numerical and model should have similar thrust EVEN in the forward flight regime.

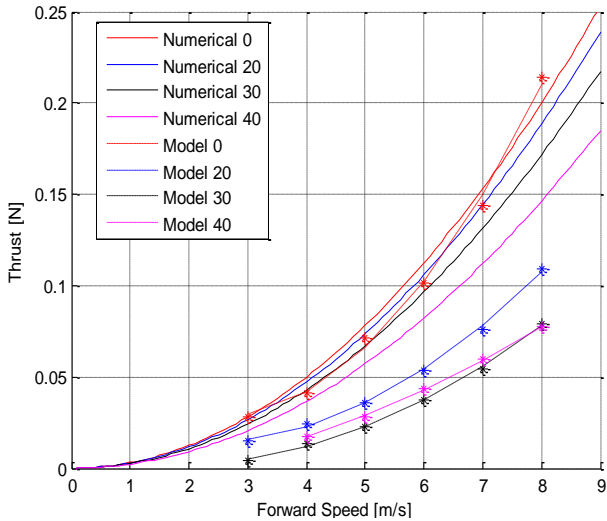


Figure 9 Graph of Thrust vs. forward speed for the two bladed natural Samara at shaft angles of 0°, 20°, 30°, 40° **Observations:** The natural Samara struggled to spin at low speeds of 1m/s to 2m/s. Only at wind speed over 3m/s, the natural Samara started to spin.

First, looking at the Natural Samara (Figure 10), at 0° shaft angle i.e. in vertical descent, the numerical and the wind tunnel test result matches, indicating that the Natural Samara is creating an effective LEV. However, as soon as the Natural Samara rotor transitions to forward flight (i.e. shaft angle ≠ 0°), the thrust drop dramatically (50% of numerical at 20° shaft angle). This may imply that the LEV is now longer present or weakened with forward flight.

The reason for loss in the thrust is potentially due to restraint in the coning, flapping and pitch angle – when a Natural Samara falls, it auto-rotates at the most natural angle. But in the wind tunnel test, the tightly hinged root meant that the Samara wings were held at an undesirable angle where autorotation is less optimal. The friction and the highly stiff wing made the seed even harder to spin. As a result, the natural Samara failed to spin at 50° shaft angle. The artificial Samaras with its greater flexibility from the balsa

wood feared much better, for all of them operated up to 80° and thus the artificial Samaras produced higher thrust than the natural in the forward flight regime.

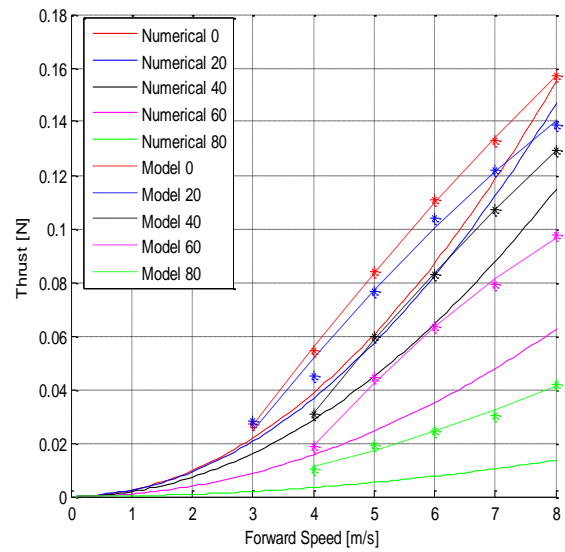


Figure 10 Graph of Thrust vs. forward speed for the two bladed 1:1 artificial Samara at shaft angles of 0°, 20°, 40°, 60°, 80° **Observations:** Much better rotation in comparison to the Natural Samara. The artificial 1:1 Samara rotor also managed to auto-rotate at shaft angles of up to 80°

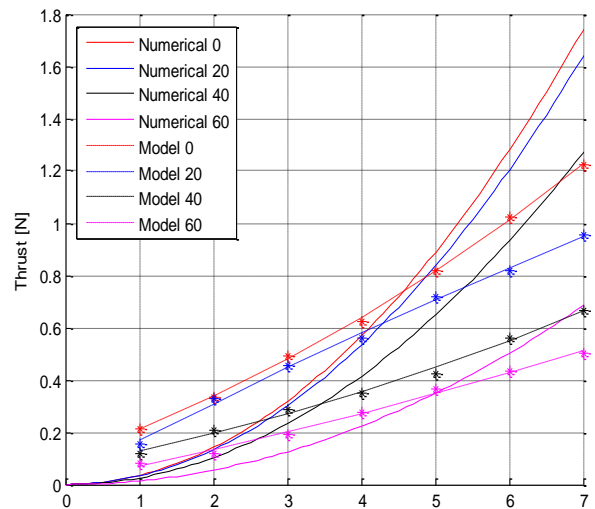


Figure 11. Graph of Thrust vs. forward speed for the two bladed 4:1 artificial Samara at shaft angles of 0°, 20°, 40°, 60° **Observations:** The artificial Samara rotor being too flexible and lengthy in span, bent a lot resulting in a huge coning angle. The deviations in 'Strain gauge reading' was large especially at high velocities, giving error of up to 0.1N for 7m/s wind speeds

As for the artificial Samaras (Figure 11, Figure 12, Figure 13), the thrust obtained in the wind tunnel test was marginally greater than the numerical for all shaft angles (except for 4:1 scale for speeds above 4m/s). This implies that

the 1:1, 4:1 and 8:1 man-made Samaras all creates LEV that surpasses those of the Natural Samara in forward and vertical flight. However, this contradicts the drop test, where the 8:1 scale Samara was viewed to have lost the LEV. Thus, it is most likely that this 'extra thrust' that is visible across all artificial rotors is from a different source other than the LEV.

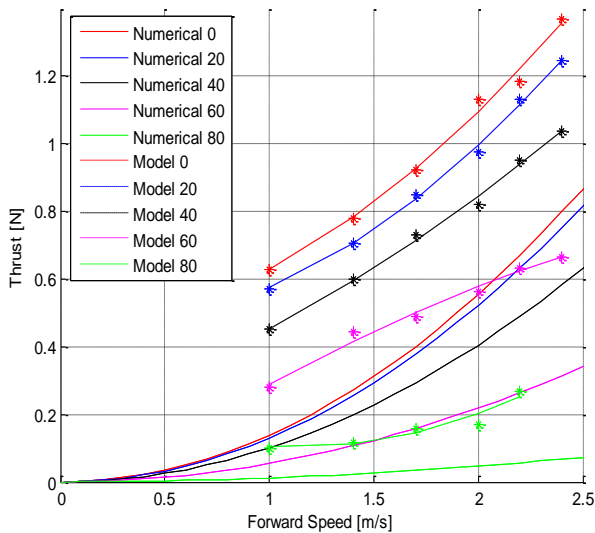


Figure 12 Graph of Thrust vs. forward speed for the two bladed 8:1 artificial Samara at shaft angles of 0°, 20°, 40°, 60°, 80°. **Observations:** Like the 4:1, the 8:1 suffered from high coning angles, thus supporting structure was placed along the wing to give more stiffness to the wing. Again the deviations in 'Strain gauge reading' was large, accounting up to 0.15N for speeds of around 2.4m/s

One of the most likely explanation to this 'extra thrust' is the pitch angle, twist and camber settings. The numerical code had a specific pitch and twist taken from the Yasuda's report. (-1.17 degrees in pitch) However, for the experimental Samara models, controlling these parameters accurately was hard. Thus, a difference between the pitch, twist existed between the numerical and experiment. In the wind tunnel test, a slight pitch up and twisting the wing tip up showed a huge jump in the 'strain gauge readings'. Thus, it is very likely that for the artificial models, a higher pitch angle was set up prior to testing.

One other contribution possible is the direct thrust from the wind. The 'strain gauge reading' comprises primarily the thrust from the rotors, but it also includes the pressing force by the wind. This results in extra reading or thrust. However,

this factor alone is not significant enough to create such difference for model and numerical.

#### Relationship between thrust and forward velocity – Is it linear or quadratic?

Based on the theory of rotor dynamics, the thrust of a rotor is proportional to  $V^2$ . This statement is true for all numerical results whether it is natural or artificial and for all shaft angles. However, for the wind tunnel test, the 1:1 (Figure 11) and 4:1 (Figure 12) showed a more linear relationship. The 4:1 especially shows a clear linear trend, where there are no dramatic quadratic increase in the thrust with higher speed.

One explanation for this lack of thrust at high speed is friction. With high speed, the load and the rate of rotation increases and this enhances the friction between the rotor head and the soldered joint. This friction can slow down the rotor significantly, resulting in a lower thrust. The other reason maybe excessive flapping and coning angle leading to blade stall. Rapid vibration and highly bent wings of the 4:1 scale Samara rotor was a clue, indicating that such blade stall may have occurred. On the other hand, the 8:1 scale Samara rotor shows a more quadratic relationship. However, this is relatively at low speeds and thus, whether the relationship will be quadratic for high speed is unknown.

#### Effects of Scaling the Rotor?

Figure 13 illustrates how the thrust curves become steeper as the Samara model is scaled from 1:1 to 4:1 to 8:1. Steeper curve or bigger gradient implies that thrust rises with bigger amount with bigger rotors. To answer 'by what factor is the thrust is being increased when scaling from 4:1 to 8:1 or etc.', the equation for each trend line was found. By dividing the gradient of the trend line with each other, the factor at which the thrust increases for each shaft angle can be found. For example,

$$\frac{\text{Gradient of 8:1 at } 0^\circ}{\text{Gradient of 4:1 at } 0^\circ} = \frac{0.5597}{0.169} = 3.31$$

So the thrust increases by 3.31 times if the wing is scaled from 4:1 to 8:1 at 0° shaft angle.

Table 4 contains the results for several different angles. Looking at the area ratio, lift should have increased by 16 times when transitioning from 1:1 to 4:1 scale. However, thrust have increased by only around 8 times. This implies the 4:1 scaled Samara wing is not producing as much thrust as expected. This may be due to loss of LEV due to partial stall.

Angle	1:1→ 1:4	1:4 → 1:8
0 degrees	×9.39	×3.31
20 degrees	×8.56	×3.64
30 degrees	×7.10	×4.31
50 degrees	×6.25	×4.12
Area Ratio	×16	×4

Table 4. Table illustrating the thrust factor obtained by scaling two bladed artificial Samara rotor

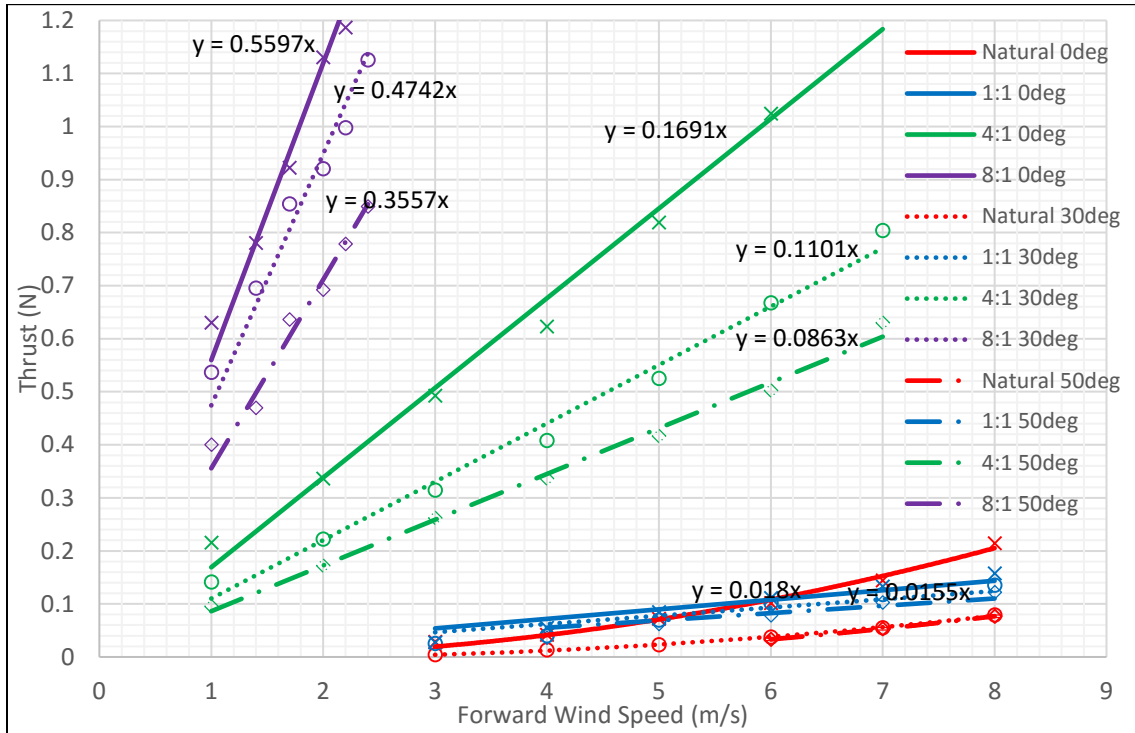


Figure 13. Graph showing the changes in the thrust with scaling.

#### 4 Conclusion

In this study, the two question – ‘Does scaling up the natural Samara degrades its aerodynamic performance?’ and ‘How does the scaled Samara performance change in the forward flight regime?’ was investigated.

Firstly, from the drop test, it was found that once the Samara reaches 8:1 scale (30cm span), a huge increase in the vertical descent was experienced suggesting that the LEV disappears. However, more accurate drop test must be carried out as there is a high chance that this may be due to underperforming scaled Samara models or the fact that the 8:1 scale wing has not reached the auto-rotational regime.

As for the wind tunnel test, for relatively low shaft angles (i.e. close to vertical descent) of around 10° to 20°, the reduction in the thrust had been small for 1:1, 4:1 and 8:1 scale artificial rotors. But as soon as the shaft angles reached beyond 30° (i.e. more forward regime), a huge drop in the thrust was observed. As for the natural Samara, as soon as the rotor transitioned to forward flight (i.e. shaft angle > 0), a huge drop in the thrust was noticed. This was likely due to the restriction of angle by the hinge joint and the effect of friction.

The artificial Samaras also produced a much higher thrust than the numerical for all shaft angles and wind speed. The more likely cause of this ‘extra thrust’ was the higher pitch angle and twist setting for the artificial rotors. Again, to fully prove the existence of LEV in forward flight, one

must find a way to control the pitch and twist settings of artificial Samaras.

Not all the rotors showed the quadratic trend expected for thrust versus forward speed. The 4:1 artificial Samara showed a strong linear relationship. This meant at high velocities, less thrust was produced than expected and this was presumably due to friction or blade stall.

The effect of scaling artificial wing from 1:1 to 4:1 was also found to boost the thrust by around 7-8 times (expected 16 times) for all shaft angles whereas scaling from 4:1 to 8:1 increase the thrust by 4 times (expected 4 times). This suggested that the 4:1 scale Samara rotor is underperforming i.e. not producing as much thrust and this implies even the 4:1 scale artificial rotor is producing an ineffective LEV.

In order to fully understand the existence of LEV when the Samara seed is scaled and travelling in forward flight. Some further improvements must be made.

Firstly, a better more optimised wing that mimic the natural seed should be made. Frictionless testing will also help, in addition to a rotor head that allows more freedom in coning, pitch and feathering angle. The wind tunnel experiment could be repeated with rate of rotation measured. This will allow the calculation of parameters like the coefficient of thrust and lift which will be important in determining the presence of the LEV. It will further give hint to whether spanwise flow that stabilise LEV is taking place or not.

## 5 References

- [1] L. Shin, "Science Scope, Lockheed martin debuts maple seed inspired drone," 19 April 2016. [Online]. Available: <http://www.smartplanet.com/blog/science-scope/video-lockheed-martin-debuts-maple-seed-inspired-drone/>.
- [2] Ulrich, Evan R., Darryll J. Pines, and J. Sean Humbert;, "From falling to flying: the path to powered flight of a robotic samara nano air vehicle," *Bioinspiration & biomimetics*, vol. 5, no. 4, 2010.
- [3] Lentink, D and Dickinson, H,M., "Rotational accelerations stabilize leading edge vortices on revolving fly wings," *Journal of Experimental Biology*, vol. 212, no. 16, pp. 2705-2719, 2009.
- [4] Thakoor, Sarita, et al, "Bioinspired engineering of exploration systems for NASA and DoD," *Artificial life*, vol. 8, no. 4, pp. 357-369, 2002.
- [5] D. S. Green, "The terminal velocity and dispersal of spinning samaras.," *American Journal of Botany*, pp. 1218-1224, 1980.
- [6] Lentink, David, et al., "Leading-edge vortices elevate lift of autorotating plant seeds," *Science*, vol. 324, no. 5933, pp. 1438-1440, 2009.
- [7] Ladera, Celso L., and Pedro A. Pineda, "The physics of the spectacular flight of the *Triplaris* samaras," *Lat. Am. J. Phys. Educ*, vol. 3, no. 3, pp. 557-610, 2009 .

- [8] R. D. Lorenz, *Spinning flight: dynamics of Frisbees, boomerangs, samaras, and skipping stones*, Springer, 2009.
- [9] Usherwood, James R., and Charles P. Ellington, "The aerodynamics of revolving wings I. Model hawkmoth wings," *Journal of Experimental biology*, vol. 205, no. 11, pp. 1547-1564, 2002.
- [10] Birch, J.M and Dickinson, M.H, "Spanwise flow and the attachment of the leading-edge-vortex on insect wings," *Nature*, vol. 412, pp. 729-733, 2001.
- [11] Birch, J, Dickson, W, and Dickinson, M.H, "Force production and flow structure of the leading edge vortex at high and low Reynolds numbers," *Experimental Biology*, vol. 207, pp. 1063-1072, 2004.
- [12] Salcedo. E, Trevino. C, Vargas. R. O, "Stereoscopic particle image velocimetry measurements of the three-dimensional flow field of a descending autorotating mahogany seed," *The Journal of Experimental biology*, vol. 216, pp. 2017-2030, 2013.
- [13] Limacher, E, and Rival, D., "On the distribution of leading-edge vortex circulation in samara-like flight," *Journal of Fluid Mechanics*, vol. 776, pp. 316-333, 2015.
- [14] A. Azuma and K. Yasuda, "Flight Performance of Rotary Seeds," *Journal of Theoretical Biology*, no. 138, pp. 23–53, 1989., vol. 138, p. 23–53, 1989.
- [15] K. Yasuda and A. Azuma, "The Autorotation Boundary in the Flight of Samaras," *Journal of Theoretical Biology*, vol. 185, no. 3, p. 313–320, 1997.
- [16] Lentink, D., Dickson, W.B., Van Leeuwen and Dickinson, M.H, "Leading-edge Vortices Elevate Lift of Autorotating Plant Seeds Supporting Material," *Science*, vol. 1438, 2009.
- [17] R. Wegner, "Deciduous Trees Traditional," Wegner, Ray, [Online]. Available: [http://natureray.com/children%20and%20nature\\_034.htm](http://natureray.com/children%20and%20nature_034.htm). [Accessed 14 7 2016].
- [18] George V. Lauder, "Aerodynamics: Flight of the robofly," *Nature*, vol. 412, pp. 688-689., 2001.

## ACKNOWLEDGMENT

I would like to thank...

Dr Djamel Rezgui  
 Dr Steve Burrow  
 Sergio  
 Ian  
 Clive  
 William Clark  
 Zaw Hike  
 Jeeah Ryu